PERMEABILITY CHARACTERIZATION OF POROUSPREFORM DURING VARTM USING FRACTALS

Debabrata Adhikari[1], Suhasini Gururaja[2]

[1]Garduate Student, Aerospace Engineering, Indian Institute of Science, Bangalore, India.
Email: debabrataa@iisc.ac.in
[2]Associate Professor, Aerospace Engineering, Indian Institute of Science, Bangalore, India.
Email: suhasini@iisc.ac.in

Keywords: Permeability, Compaction Pressure, Fractals, Tortuosity.

Abstract
Accurate characterization of permeability of the complex architecture of porous preform is the first step towards efficient and cost-effective resin impregnation to yield composite parts via vacuum assisted resin transfer molding (VARTM). Determination of preform permeability in different directions is inherently dependent on the available pore spaces in the complex labyrinth of the fabric layup. A major challenge is to understand the pattern of disordered complex microstructure and a quantitative description of permeability as a function of local porosities. Depending on the fiber alignment, several models have been developed to determine permeability as a function of fiber volume fraction by means of flow thorough ordered compacted parallel and perpendicular channels. It was observed that in most cases, experimentally determined permeability fitted well with the classical permeability porosity relation of Kozeny-Carman (KC) model with an empirical Kozeny constant as a fitting estimate. KC model shows that as the fiber volume fraction decreases the permeability increases; however, results indicate that in some cases, this behavior is not exhibited.

Detailed permeability experiments conducted on carbon fiber preform YC200 (Fibertech Co. Ltd.) show that as the fiber volume fraction increases, the permeability along the fiber direction increases; the converse was found to occur for permeability experiments conducted on the fabric in the transverse direction. Once the fiber layups are stacked together, diameter of micro pores and capillary channels do not behave like perfectly aligned parallel micro channels. There is considerable disorder in the preform microstructure in terms of different capillary diameters, length of the tortuous capillaries between tows, spacing between individual filaments within a single tow, and the spacing between stitching threads of the fabric, etc. In the present study, two separate unit cell models have been developed with and without a combination of pore area fractal dimension and tortuosity. Predicted results a good agreement with the experimentally determined permeability in both the longitudinal and transverse directions.

1. Introduction

Liquid composite molding (LCM) processes involve the impregnation of liquid resin to saturate the porous cavities of the dry fiber preform. The resin transfer molding (RTM), structural reaction injection molding (S-RIM), Seemann's composite resin transfer molding process (SCRIMP), vacuum induced preform relaxation (VIPR), VARTM etc. belongs to the class of LCM processes. Ideally, in all the processes impregnation of dry preform is accomplished due to created pressure gradient in presence of highly viscous resin. In last few decades, VARTM process has received considerable attention due to its low initial investment, low labor cost, room temperature and ease in manufacturing

large components. Researchers mostly focus on the ability to predict the process parameters and flow physics during impregnation and ultimately to achieve a consistent product.

VARTM is a modified open mold process wherein resin saturates available pore spaces of fiber preform due to the pressure gradient created by the vacuum pump. A schematic of vacuum infusion is shown in the figure (Fig.1). The degree of vacuum pressure determines the size and distribution of pores through the structure that may lead to dry spots and micro voids. Influence of pressure gradient cause the changes of fiber volume fraction that will affect the permeability of the fiber layup. As the flow front advances, three regions are created, namely, fully saturated, partially saturated and dry region. Additionally, the compaction pressures in the porous fiber preform also vary as the flow front advances resulting in spatially varying porosities. This results in a varying permeability of the preform during VARTM.

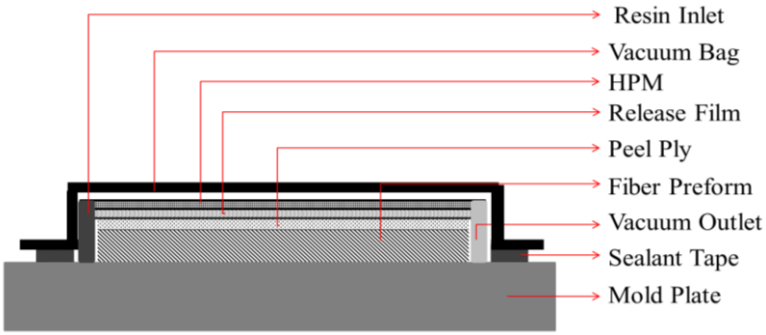

Figure 1. Schematic of VARTM infusion

In the past, several studies have been conducted to characterize permeability through experiments as well as analytical/numerical modeling. There are three major experimental approaches to characterize permeability, namely, using saturated, unsaturated and radial flow experiments. Saturated permeability experiments are mostly useful for sedimentation and percolation studies of seepage flow [1]. Unsaturated flow experiments are typically conducted by maintaining either a constant flow rate or constant pressure [2]. In both the constant flow rate and constant pressure methods, transverse and longitudinal permeability can be characterized by varying the orientation of fiber layup to the flow direction.

Preform permeability in different directions is inherently dependent on the available pore spaces in the complex labyrinth of the fabric layup. A major challenge is to understand the pattern of disordered complex microstructure and a quantitative description of permeability as a function of local porosities. Depending on the fiber alignment, several models have been developed to determine permeability as a function of fiber volume fraction by means of flow thorough compacted parallel and perpendicular channels [3]. In [5], a rectangular unit cell model was developed based on the geometry of pore area, weft, and warp of the preform. It was observed that in most cases, experimentally determined permeability fitted well with the classical permeability porosity relation of Kozeny-Carman (KC) model with an empirical Kozeny constant as a fitting estimate [2]. Further studies on KC equation indicate that the Kozeny ‘constant’ is in fact dependent on the capillaries microstructure and a function of porosity [3]. KC model shows that as the fiber volume fraction decreases the permeability increases; however, results indicate that in some cases this behavior is not exhibited. Simacek and Advani developed a permeability model based on lubrication theory to describe the flow through open channels using stokes law and flow within a tow by using Darcy’s law [4].

Once the fiber layups are stacked together, diameter of micro pores and capillary channels does not behave like perfectly aligned parallel micro channels. Boming et al. [5] developed a simplified in-plane permeability model based on two scale flow in a unit cell. Although preforms are aligned in certain order, sometimes it does not follow a periodicity in the structure of pore area, warp and weft of fiber. In that case, repeating unit cell model cannot predict the behavior of flow in the disorder

structure of pore and capillary. There is considerable disorder in the preform microstructure in terms of different capillary diameters, length of the tortuous capillaries between tows, spacing between individual filaments within a single tow, and the spacing between stitching threads of the fabric, etc. Pituchamani and Ramakrishnan presented a fractal permeability model based on the image analysis of disordered pore micro-structure [6]. However, their model shows a substantial difference compared to experimental results. Figure (Fig.2, 3) shows the transverse and longitudinal cross-sectional micro computed tomography (μ-CT) image of a cured uni-directional carbon fiber reinforced plastic (UD-CFRP) laminate along fiber direction for 4, 8 and 12 ply configuration.

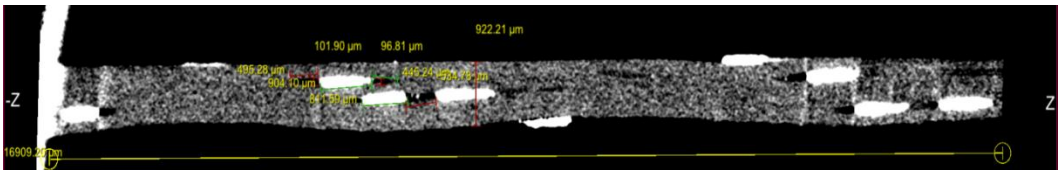

(a)

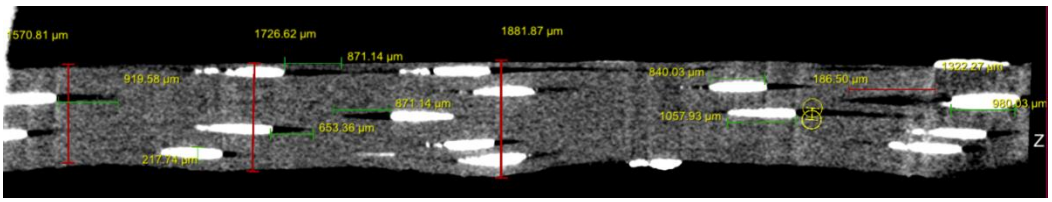

(b)

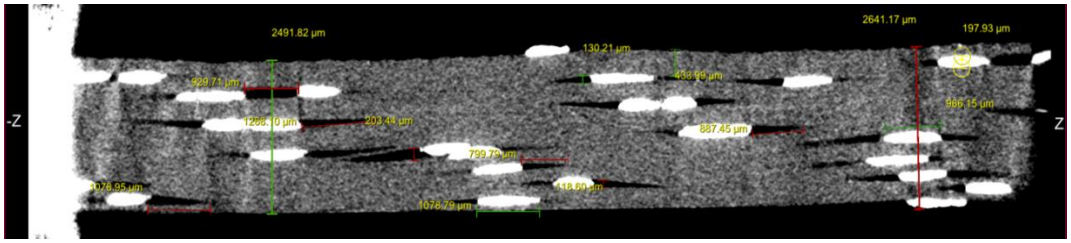

(c)

Figure 1. Longitudinal cross-section of μ-CT image for (a) 4ply (b) 8ply and (c) 12ply configuration.

Once the fiber layups are stacked together, diameter of micro pores and capillary channels does not behave like perfectly aligned parallel micro channels. There is considerable disorder in the preform microstructure in terms of different capillary diameters, length of the tortuous capillaries between tows, spacing between individual filaments within a single tow, and the spacing between stitching threads of the fabric, etc. [5-7]. Figure (Fig.1) depicts the cross-sectional micro computed tomography (μ-CT) image of a unit cell of a 12 ply uni-directional carbon fiber reinforced plastic (UD-CFRP) laminate along fiber direction. A fractal technique can be used to describe the disordered nature of pore structures for such configurations. Two fractal dimensions - one associated to the pore area fractal dimension D_f and another one associated with the tortuosity dimension D_T - are assumed. Peng et al. developed a new form of permeability model for a homogeneous porous media by means of fractal geometry of pore area fractal dimension and tortuosity of pore channel [7].

In the present study permeability with variable fiber volume fraction (or porosity), compaction experiments were conducted that correlate applied pressure and fiber volume fraction. Compaction experiments were carried out by changing the number of layers in both dry and wet conditions using a micro universal testing machine (micro-UTM). Vacuum infusion experiments have been conducted using an array of pressure sensors and digital dial gauge to capture the *in situ* transient pressure gradients during resin infusion. Consequently, the flow behavior was characterized by varying number

of layers and fiber orientation to determine the principal permeability values Kxx and Kyy. Later, two separate unit cell models were developed with and without a combination of pore area fractal dimension and tortuosity. Predicted results show a good agreement with the experimentally determined permeability in both the longitudinal and transverse direction.

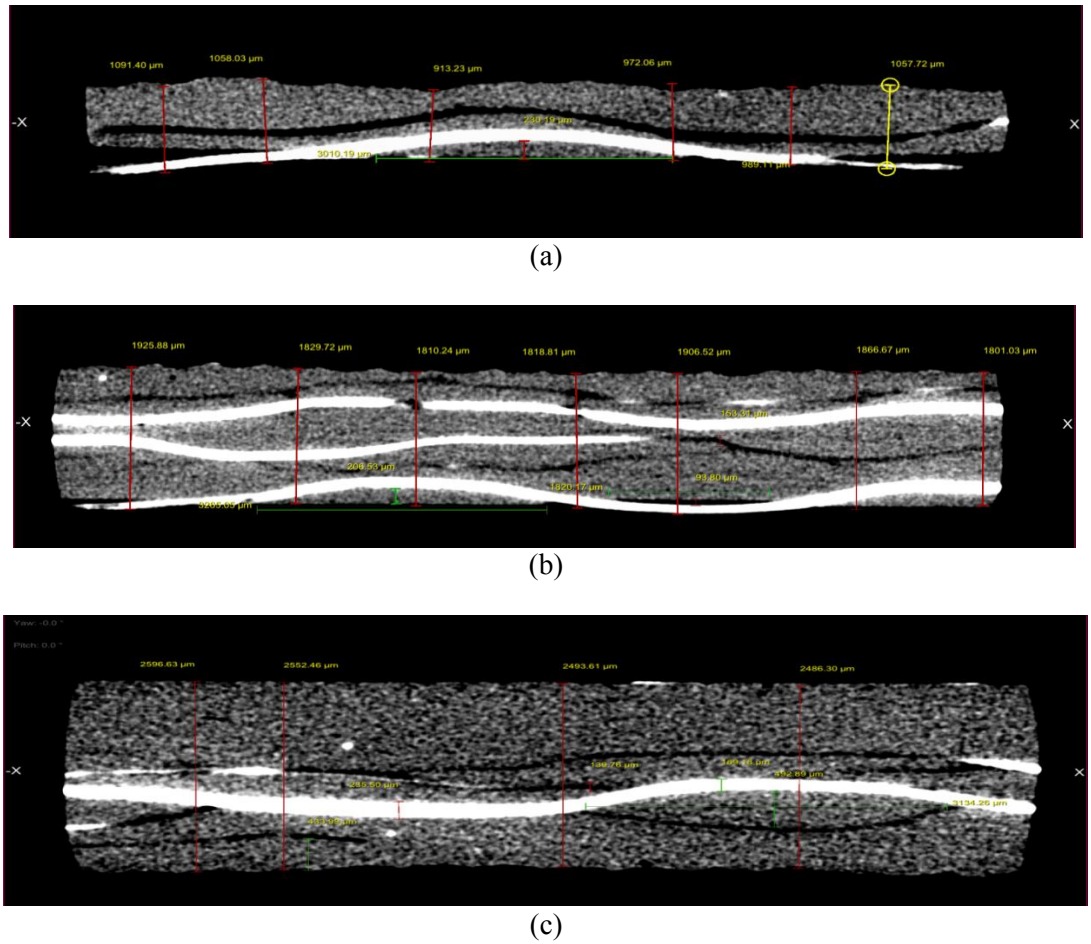

(a)

(b)

(c)

Figure 3. Transverse cross-section of µ-CT image for (a) 4ply (b) 8ply and (c) 12ply configuration.

2. Materials Used

Vacuum infusion experiments have been performed wherein the dry fabric is impregnated with liquid resin to completely saturate the preform. Line infusion experiments replicating 1-D flow have been conducted in the present study. Unidirectional carbon fiber preforms YC-N200 from Fibertech Co. Ltd. (σf: 4900 MPa, areal weight: 200$gmm2/$, and E :230 GPa) have been used for all the experiments described in this work. Based on a previous study, sugar solution of (84-86) cP viscosity has been used for all the infusion experiments [8]. A 30 mm thick transparent acrylic plate has been used as the base mold. UD carbon fabric of 300x150mm was used for all vacuum infusion experiments. A maximum vacuum pressure of (72-70) kPa was achieved using the vacuum pump. Compaction experiments were carried out with a stack of 4, 8 and 12 layer of 50 mm diameter fabric using the micro-UTM in both the dry and wet condition.

3. Fiber Compaction

An empirical power law Eq.1 has been developed by Robitaille et al. [10] relating fiber volume

fraction of the compacted preform to the initial fiber volume fraction *at* $1Pa$ pressure.

$$V_f = V_{f_o} P_{comp}^{B} \quad (1)$$

Where, B is the compacting stiffness index (B<1). The variation in thickness change $h_{(P_{comp})}$ with fibre volume fraction is given by

$$h_{(P_{comp})} = \frac{\rho_{surf}}{\rho v_f} \quad (2)$$

Fiber surface density and volume density is denoted by ρ_{surf} and ρ respectively.

Experimental data has been fitted with the power law equation-1 and extrapolated up to $1Pa$ pressure to get the compaction coefficient Vfo and stiffening index (< 1) [9]. It can be observed that as the number of plies decrease, Vf is found to increase significantly. Table 1 represents the value of the coefficients $a\ and\ B$ for both the dry and wet condition of UD layups.

Table 1. Fiber compaction

Ply Number	V_{fo}[%]at 1Pa	B
4 Ply	Dry: 8.303	0.1647
	Wet: 8.578	0.1643
8 Ply	Dry: 15.06	0.1165
	Wet: 14.94	0.1229
12 Ply	Dry: 14.08	0.1091
	Wet: 14.90	0.1049

Ply thickness of each ply can be determined using the relation Eq.2 that will be used to get the height of single fiber layer for certain fiber volume fraction.

4. Permeability characterization

Permeability is another key aspect of VARTM that corresponds to the hydraulic conductivity of fluid pass through the fibrous porous media. In 1856, Darcy proposed an empirical model for ground water seeping through the homogeneous porous column of sand as follows:

$$U = \frac{[K]}{\mu} \nabla P \quad (3)$$

Where, $[K]$ corresponds to the permeability tensor of the media, μ and ∇P corresponds to viscosity of the fluid and pressure gradient across the flow channel. The permeability tensor $[K]$ can be normalized to three principal permeability by Kxx, Kyy and Kzz depends on the direction of the flow front to the alignment of fiber orientation.

Resin flow in VARTM is a transient process. Two-phase flow scenario of saturated and unsaturated condition happens together at the flow front. Air bubbles in the dry preform are slowly pushed out by resin as infusion progresses. This process occurs in two steps: firstly, the air bubbles are replaced by resin in the gaps between two tows (inter tow region) while the air bubbles are replaced by resin at a slower rate within the tow (intra tow region). Thus, during this process, there is a mismatch of flow front into the inter and intra tow regions of the fabric. Therefore, there is a continuous variation of porosity in the preform as the resin flow progresses [9].

A novel method was developed to calculate the permeability under varying fluid pressures and associated variations in porosities characteristic to VARTM. It was observed from compaction experiments that fiber volume fraction varies with the number of plies. As the pressure field is no

longer linear along the flow direction, one can establish the Darcy's law locally in such a way that it can corresponds to the local pressure drops across partially saturated region.

$$\frac{dl(t)}{dt} = \frac{K}{\mu\varphi}\frac{dP}{dl} \tag{4}$$

Here, $dl(t)$ represents the transient variation of flow front, K is the scalar permeability (since 1D flow is assumed), φ is porosity, and dP implicitly accounts for compaction pressure variation at the flow front to the pressure of previous wetted region. Therefore, $l(t)$ and φ will vary with the compaction pressure, accordingly.

Three sets of experiments have been conducted to get a range of permeability values K with V_f by varying the number of fiber layups in $0^o$and 90^oorientation with respect to the direction of flow front to the fiber tow direction. Figure 5 shows the permeability data obtained from experiments fitted with the well-known Kozeny-Carman equation for 90^o orientation of fiber.

4.1 Unit Cell Model

Although fiber preform microstructures shows considerably disordered nature of wefts, warps and channels (or gaps) due to the in-plane displacement of stacking disordered of multiple layers of fiber preform. It is possible to find an analytical model for permeability based on the concept of a unit cell. Simacek and Advani [11] represent unit cell geometry for a well packed parallel fiber. It is unable to get an analytical model for irregular geometry. Boming et al. [5] developed a typical analytical model for plane weave fabric by considering three domains consists of the warps, wefts and the channel or gap. In their model warp and weft are the crossed fiber tow consist of thousands many parallel filaments. In out model we have adopted the same idea of warp, weft and channel. We have defined weft as the stitching thread of the preform and warp is the parallel fiber. A typical cross sectional of a unit cell has shown in the Figure 4.

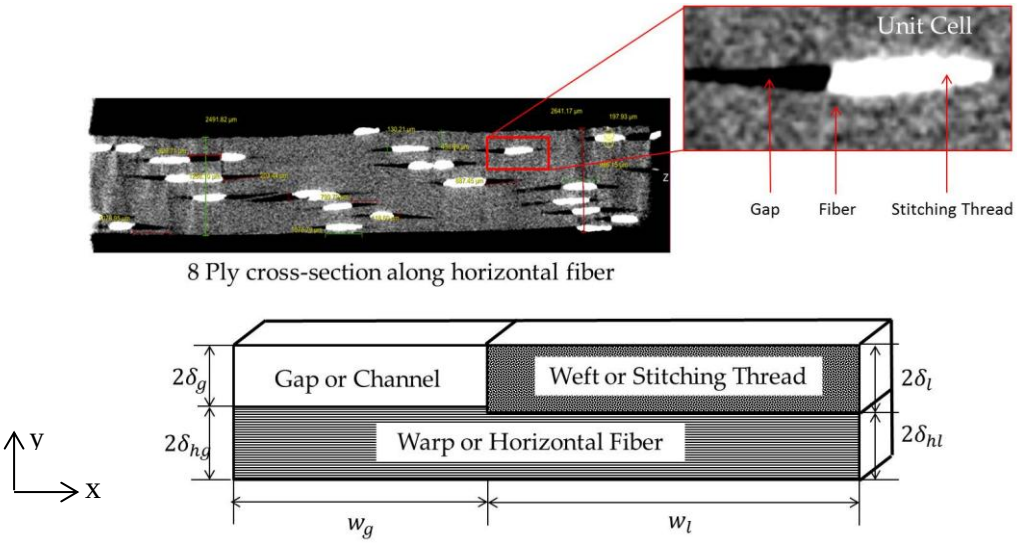

Figure 4. Unit cell for transvers fiber to the flow direction

From the model equation of Boming et al. [5], a modified effective permeability of unit cell can be derived as the sum of all the permeability through the gap or channel, weft and warp region.

$$K_{yy,\ eff} = \frac{a_g}{A}K_g + \frac{a_h}{A}K_h + \frac{a_l}{A}K_l \tag{5}$$

Where,

$K_{yy,\ eff}$ = Effective transverse permeability

K_g= Permeability in the gap or channel

K_l= Permeability in the weft region.

K_h = Permeability in the warp region of perpendicular fiber to flow direction

Total area A = a_g(area in the gap) + a_h(area in the warp) + a_l(area in the weft region)

It is observed that as the gap or channel is along flow direction, it is reasonable to undertake the unit cell model to estimate the effective permeability. It is also noted that fiber of YC-N200 weft is a combination of highly packed glass thread; therefore, the volume fraction of stitching thread is assumed to be 0.9-0.95 so that it behaves like a solid block. Transverse permeability in the gap for 4, 8 and 12 ply is about 100 times higher than the permeability in the warp region. Average value of $K_{yy,\ eff}$ is obtained from different position of unit cell. Effective permeability is compared with the experimentally determined transverse permeability for 4, 8 and 12 ply configuration. The results show a good agreement with the experiment in Figure 5.

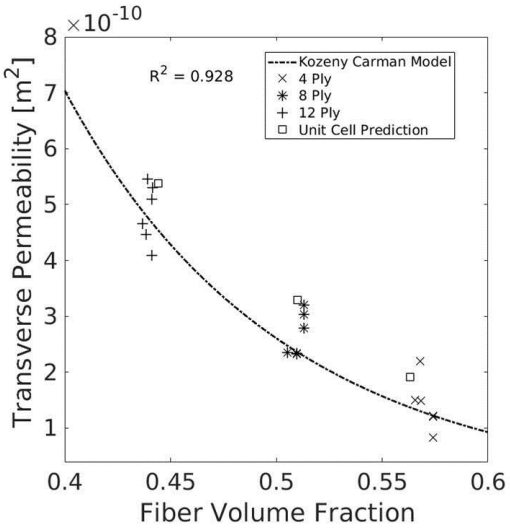

Figure 5: Transverse permeability using unit cell approach

4.2 Fractal Permeability Model

From the cross-sectional view of YC-N200 along thread direction, warp is considered as stitching thread and weft is considered as the fiber tows. Therefore, the gap or channel and warp of the preform become perpendicular to the flow direction whereas fiber tows are along the flow direction. Although flow in the gap or channel is much faster compared to fiber tow, it does not help to improve the higher permeability in the longitudinal direction for flow. It is observed that as the flow front advances along the fiber tow, it will encounter the stitching thread and the associated gap or channel perpendicular to it so that flow will get hindered by the stitching thread many times. Although there fiber tow and stitching thread are placed parallel in a single ply, various compaction pressure and different stacking of multiple layer cause a considerable disordered in the gap or pore channel, stitching thread and fiber tow.

Ketz and Thompson [12] first present the experimental observation of fractals nature in sandstone samples. The disordered nature of pore microstructure offers the existence of fractal characteristic formed by the pores and tortuosity of the capillaries. Therefore, applying fractal theory to a cumulative size of pore distribution in porous media, we get the fractal dimensions as follows:

$$N(\varepsilon \geq \lambda) = \left(\frac{\lambda_{max}}{\lambda}\right)^{D_f} \tag{6}$$

Where N is the total number of pore or capillaries in an area of ε, whose diameter is greater or equal to the pore diameter of $\boldsymbol{\lambda}$ whereas λ_{max} corresponds to the maximum porssible diameter of pore. If the dimension $1< D_f < 2$ satisfies the relation the porous structure qualifies for the fractal in two dimensions.

Similarly, a porous media with different pore size can be considered as the boundless of tortuous capillary tubes in various cross-section areas with a diameter λ of tortuous tube $L_t(\lambda)$ to the straight length L_o. Wheatcraft and Tyler [13] proposed a the model to describe the tortuous nature of the capillary by the scaling law

$$L_t(\delta) = \delta^{1-D_T} L_o^{D_T} \tag{7}$$

Where δ corresponds to the length scale of measurement and D_T is the tortuosity fractal dimensions.

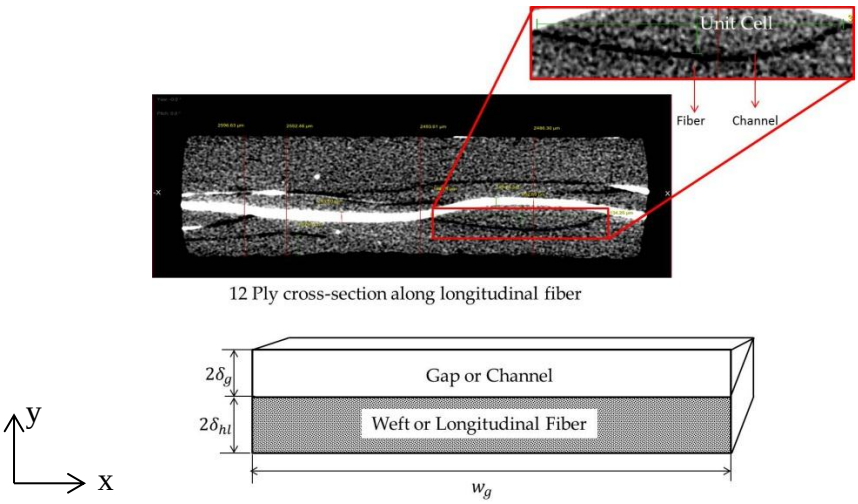

Figure 5. Disordered unit cell for longitudinal fiber to the flow direction

Pore of area fractal dimension D_f of channel or gap has been estimated from the cross-section view along longitudinal fiber whereas tortuosity fractal dimension of pore channel from the cross-section view along transverse fiber direction of channel. Box counting method has been adopted to estimate the fractal dimension by varying number of square pixel. Fractal dimension of 4, 8 and 12 ply for the channel and fiber has shown in the Table-2.

Once the fractal dimension has determined effective permeability in the gap and weft region of the unit cell has been estimated using the relation [7]

$$K = \frac{\pi}{128} \frac{{L_o}^{1-D_T}}{A} \frac{D_f}{3+ D_T+ D_f} \lambda_{max}^{3+D_T} \tag{8}$$

Table 2. Fractal Dimension cross-section perpendicular to flow direction

	Longitudinal direction		Transverse direction	
Ply Configuration	D_f	D_T	D_f	D_T
4 Ply	1.5174	1.86	1.4836	1
8 Ply	1.4036	1.92	1.52	1
12 Ply	1.3367	1.877	1.815	1

Where A and λ_{max} has been determined from the relation of unit geometry for the gap region and compaction properties of fiber preform for the weft region in a tow.

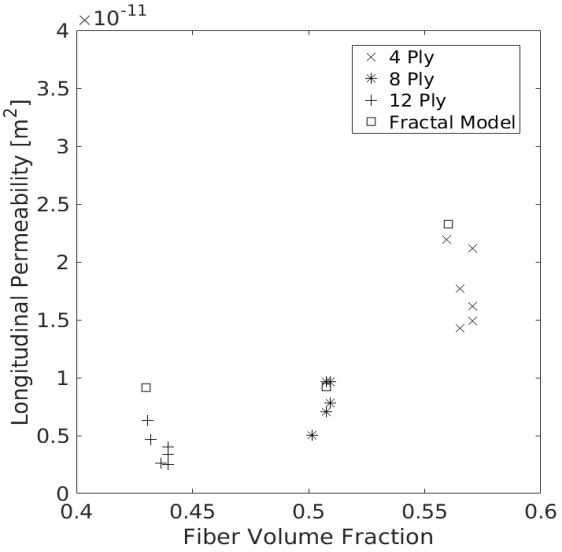

Figure 6: Longitudinal permeability using unit cell approach

Later the effective permeability has been determined using the relation

$$K_{xx,\ eff} = \frac{a_g}{A} K_g + \frac{a_{hl}}{A} K_{hl} \tag{9}$$

Effective permeability determines with combination of fractal approach and unit cell show a good agreement to capture the inverse phenomenon of preform permeability to the conventional Kozeny Carman model. Therefore the fractals and micro-structural approach has an ability to predict the behavior of dual nature of permeability with fiber volume fraction.

5. Conclusions

Permeability variation with porosity for a C-fiber preform has been presented in the current work. The following conclusions can be drawn:

1. A novel method for permeability measurement from fluid pressure data has been presented.

3. Compaction experiments under dry and wet conditions have been carried out that demonstrate the behavior of the porous preform and an additional input to determine the maximum λ under applied pressure (compaction).
4. Experimentally determined transverse permeability K_{yy} was found to follow the trend captured by the well-known Kozeny Carman relation. It has been validated with the unit cell approach.
5. Fractal permeability model has been developed to capture disordered nature of porous structure using box counting method of computed tomography image of cured laminate.
6. Unit cell model with fractal dimension are able to capture the inverse nature of experimentally determine longitudinal permeability K_{xx}.

The use of these permeability models will be very helpful in the complete numerical development of fluid flow during VARTM processing.

Acknowledgments

The authors acknowledge the support of AFMM center of IISc Bangalore to avail the facility to conduct the micro computed tomography of cured laminate.

References

[1] D. W. Taylor, Fundamentals of soil mechanics, *Soil Science* 66 (2) (1948) 161.

[2] D. J. Gunn, A. R. Aitken, *Canadian Journal of Chemical Engineering*, 39, 1961, pp. 209-14.

[3] Y. Lai, B. Khomami, J. L. Kardos, Accurate permeability characterization of preforms used in polymer matrix composite fabrications processes, *Polymer composite*, June 1997, Vol. 18, No. 3, pp. 368-77.

[4] P. Simacek and S.G. Advani, *Polymer Composites*, 19, 626, 1988.

[5] B. YU and L. James Lee. A simple in-plne permeability model for textile fabrics. *Polymer Composite, Vol. 21, No. 5,* October 2000.

[6] R. Pitchumani and B. Ramakrishnan. A fractal geometry model for evaluating permeability of porous preforms used in liquid composite molding*, International Journal of Heat and Mass Transfer, 42, pp.* 2219-2232, 1999.

[7] P. Xu and B. Yu. Developing a new form of permeability and Kozeny-Carman constant for homogeneous porous media by means of fractal geometry. Advances in Water Resources, Vol.31, pp. 74-81, 2008.

[8] C. Arulappan, A. Duraisamy, D. Adhikari, S. Gururaja, Investigations on pressure and thickness profile in carbon fiber-reinforced polymers during vacuum assisted resin transfer molding, *Journal of reinforced plastics and composites*, pp.1-16, Dec 2014.

[9] D. Adhikari, S. Gururaja, Characterisation of permeability and compaction behavior for different fiber layups during VARTM, International Conference on Composite materials and structures, Paper ID 380, 27-29 December 2017.

[10] F. Robitaille and R. Gauvin. Compaction of textile reinforcements for composites manufacturing. i: Review of experimental results". *Polymer composites,* 19(2), pp. 198–216.

[11] P. Simacek and S. G. Advani. *Polymer Composite*. 17, 887 (1996).

[12] Katz. AJ, Thomson AH. Fractal sandstone pores: automated measurements using Scanning-microscope images. *Physical Review B* ; 33:6366-44, 1986.

[13] Wheatcraft SW, Tyler SW. An explanation of scale-dependent dispersivity in heterogeneous aquifers using concepts of fractal geometry. *Water Resources Res*, 24:566, 1988.